A Unique Framework in $BaGa_2Sb_2$: A New Zintl Phase with Large Tunnels

Sung-Jin Kim† and Mercouri G. Kanatzidis*

Department of Chemistry and Center for Fundamental Materials Research, Michigan State University, East Lansing, Michigan 48824

Received January 18, 2001

$BaGa_2Sb_2$ was obtained from a direct element combination reaction in a sealed graphite tube at 950 °C, and its structure was determined by single-crystal X-ray diffraction methods. It crystallizes in the orthorhombic space group *Pnma* (No. 62) with $a = 25.454(5)$ Å, $b = 4.4421(9)$ Å, $c = 10.273(6)$ Å, and $Z = 8$. The anionic $[Ga_2Sb_{6/3}]^{2-}$ framework is assembled by the ethane-like dimeric $[Sb_3Ga-GaSb_3]$ units sharing Sb atoms, forming parallel tunnels with a 26-membered ring cross section. These tunnels are filled with Ba atoms. The three-dimensional $[Ga_2Sb_{6/3}]^{2-}$ framework features a new structure type. The compound satisfies the classical Zintl concept. Band structure calculations indicate that the material is a semiconductor, and this is confirmed by spectroscopic experiments which show $E_g \sim 0.35$ eV. The calculations also suggest that the structure is stabilized by strong Ga−Ga covalent bonding interactions. Polycrystalline ingots of $BaGa_2Sb_2$ show room-temperature electrical conductivity of ∼65 S/cm and a Seebeck coefficient of +65 μV/K.

Introduction

Zintl phases with complex anionic frameworks and heavier elements are expected to be narrow-gap semiconductors and may have useful electronic properties provided they are environmentally stable. It is believed that the electrical properties of Zintl phases could be tuned by the selection of elements involved in the anionic frameworks. Recently, several new air-stable Zintl anisotropic frameworks have been reported including the ternary phases $Yb_{14}MnSb_{11}$,[1] $Ba_8In_4Sb_{16}$,[2] $Ba_2Sn_3Sb_6$,[3] and $SrSn_3Sb_4$.[4] $Ba_8In_4Sb_{16}$ is a p-type narrow band gap semiconductor with holes delocalized over the Sb sublattice. $Ba_2Sn_3Sb_6$ and $SrSn_3Sb_4$, however, show metallic behavior that could arise from either increased orbital overlap resulting high bandwidths and negative band gaps (bottom of conduction band below top of valence band) or inadvertent doping which is difficult to avoid.[5] Our attempts to synthesize new Zintl phases with narrow band gaps and complex structures[2] resulted in the discovery of $BaGa_2Sb_2$ which features a unique framework. That a novel phase with a relatively simple stoichiometry has been discovered, after several decades of ongoing exploratory investigations in Zintl type compounds, is surprising. This implies that much remains to be learned in terms of new phases where the emphasis should be placed in compounds with good environmental stability and with an eye for practical applications. In this paper we describe the synthesis, crystal structure, spectroscopic characterization, electrical transport properties, and electronic structure of $BaGa_2Sb_2$.

* To whom correspondence should be addressed. E-mail: Kanatzid@cem.msu.edu. Tel: 517-353-0174.

† Permanent address: Department of Chemistry, Ewha Woman's University, Seoul, Korea 120-750.

(1) Chan J. Y.; Olmstead M. M.; Kauzlarich S. M.; Webb, D. J. *Chem. Mater.* **1998**, *10*, 3583−3588.
(2) (a) Kim, S.-J.; Hu, S.; Uher, C.; Kanatzidis, M. G. *Chem. Mater.* **1999**, *11*, 3154.
(3) Chow, D. T.; McDonald, R.; Mar, A. *Inorg. Chem.* **1997**, *36*, 3750.
(4) Lam, R.; Mar, A. *Inorg. Chem.* **1996**, *35*, 6959.
(5) Lam, R.; Zhang, J.; Mar, A. *J. Solid State Chem.* **2000**, *150*, 371.

Experimental Section

Synthesis. The crystal used in the structure determination resulted from the reaction of a mixture of three elements (Ba, Aldrich, chunk under oil, 99%; Ga, Cerac, shots, 99.999%; Sb, Cerac, chips, 99.999%) in a ratio of Ba:Ga:Sb = 0.1373 g (1 mmol):0.2092 (3 mmol):0.3653 g (3 mmol). The reaction mixture was handled in a nitrogen-filled glovebox. It was placed in a graphite tube and sealed in an evacuated silica tube (9 mm i.d). The sealed mixture was heated slowly up to 950 °C for 2 days, kept at that temperature for 1 day, and subsequently cooled to room temperature over 1 day. The reaction led to the formation of a few rod-shaped black crystals along with gray featureless pieces. Semiquantitative microprobe analysis on single crystals gave $Ba_{1.0(2)}Ga_{1.9(2)}Sb_{2.0(2)}$ (average of three data acquisitions). Once the stoichiometry was determined from the X-ray single-crystal structure analysis, $BaGa_2Sb_2$ was prepared rationally as a single phase, starting from the exact stoichiometric ratio and using the same temperature profile and similar reaction vessel. The X-ray powder pattern of bulk samples agreed well with the powder pattern calculated from the single-crystal parameters.

Electron Microscopy. Semiquantitative microprobe analysis of the compounds was performed with a JEOL JSM-35C scanning electron microscope (SEM) equipped with a Tracor Northern energy dispersive spectroscopy (EDS) detector. Data were acquired using an accelerating voltage of 20 kV and a 30 s accumulation time.

Differential Thermal Analysis. Differential thermal analysis (DTA) was performed with a Shimadzu DTA-50 thermal analyzer. The ground sample (∼30.0 mg total mass) was sealed in a carbon-coated silica ampule under vacuum. A silica ampule containing alumina of equal mass was sealed and placed on the reference side of the detector. The sample was heated to 950 °C at 10 °C/min and isothermed for 10 min, followed by cooling at −10 °C/min to 50 °C. The stability and reproducibility of the sample were monitored by running multiple heating and cooling cycles. The residue of the DTA experiment was examined with X-ray powder diffraction.

Infrared Spectroscopy. Infrared diffuse reflectance spectra of $BaGa_2Sb_2$ were recorded to probe the presence of a band gap. The sample was ground into a powder prior to the data acquisition. The spectra were recorded in mid-IR region (4000−400 cm^{-1}, 4 cm^{-1} resolution) with a Nicolet 740 FT-IR spectrometer equipped with a

10.1021/ic010069n CCC: $20.00
Published on Web 06/20/2001

Table 1. Selected Data from the Single-Crystal Refinement of $BaGa_2Sb_2$

empirical formula	$BaGa_2Sb_2$
fw	4162.24
temp (K)	293(2)
wavelength (λ(Mo Kα), Å)	0.710 73
cryst system	orthorhombic
space group	*Pnma* (No. 62)
unit cell dimens (Å)	$a = 25.454(5)$
	$b = 4.4421(9)$
	$c = 10.273(2)$
V (Å^3)	1161.6(4)
Z	8
density (ρ_{calc}) (g/cm^3)	5.950
final R indices [$F_o^2 > 2\sigma(F_o^2)$][a]	R1 = 0.0287, wR2 = 0.0710

[a] $R1 = [\sum||F_o| - |F_c||]/\sum|F_o|$. $wR2 = \{[\sum w(F_o^2 - F_c^2)^2/[\sum w(F_o^2)^2]]\}^{1/2}$. $w = \sigma_F^{-2}$.

diffused reflectance attachment. Absorbance values were calculated from the reflectance data using the Kubelka−Munk function.[6]

Electronic Structure Calculations. Electronic structure calculations were performed by the Hückel method within the framework of the tight-binding approximation.[7] The program CAESAR written by M.-H. Whangbo was used.[8] Density of states (DOS) and crystal orbital overlap populations (COOP) were calculated on the basis of 516 K point sets based on the primitive orthorhombic structure. The atomic orbital parameters employed in the calculations were default values in the CAESAR program.[9]

Crystallographic Studies. A black rod-shaped crystal with dimensions 0.03 × 0.03 × 0.20 mm was mounted on a glass fiber. A Siemens SMART Platform CCD diffractometer was used to collect intensity data using graphite-monochromatized Mo Kα radiation. The diffraction data were collected over a full sphere of reciprocal space up to 56° in 2θ. The individual frames were measured with an ω rotation of 0.3° and an acquisition time 30 s. To check the stability of the crystal at the end of data collection, the initial 50 frames of data were measured again and compared. No crystal decay was detected. The SMART software[10] was used for data acquisition, and SAINT,[11] for data extraction and reduction. The absorption correction was performed empirically using SADABS.[12] The unit cell parameters were obtained from least-squares refinement using 600 reflections chosen from a full sphere of reciprocal space up to 56° in 2θ. The observed Laue symmetry and systematic extinctions were indicative of the space groups *Pnma* or $Pn2_1a$. The centrosymmetric space group *Pnma* was assumed, and subsequent refinements confirmed the choice of this space group. The initial positions of all atoms were obtained from direct methods. The structure was refined with full-matrix least-squares techniques with the SHELXTL[13] package of crystallographic programs. Once all atoms were located, their occupancies were allowed to vary successively, but refinements did not lead to any significant change in the occupation factor. The final cycle of refinement performed on F_o^2 with 62 variables and 1455 averaged reflections converged to residuals wR2 ($F_o^2 > 0$) = 0.0745. The conventional R index based on reflections having $F_o^2 > 2\sigma(F_o^2)$ was 0.0287. The final difference Fourier synthesis map showed maximum and minimum peaks of 2.041 and −1.085 e/Å^3, respectively. The complete data collection parameters and details of structure solution and refinement results are given in Table 1. Final atomic positions and displacement parameters are given in Table 2.

Table 2. Atomic Coordinates (×10^4) and Equivalent Isotropic Displacement Parameters (Å^2 × 10^3) for $BaGa_2Sb_2$

atom	x	y	z	U(eq)[a]
Ba(1)	2074(1)	1/4	5498(1)	11(1)
Ba(2)	393(1)	3/4	7795(1)	14(1)
Sb(1)	3292(1)	1/4	8007(1)	11(1)
Sb(2)	1856(1)	3/4	8120(1)	11(1)
Sb(3)	779(1)	1/4	264(1)	10(1)
Sb(4)	704(1)	1/4	5195(1)	11(1)
Ga(1)	3187(1)	3/4	4656(1)	12(1)
Ga(2)	4212(1)	1/4	6768(1)	12(1)
Ga(3)	2857(1)	3/4	7015(1)	11(1)
Ga(4)	4650(1)	1/4	8971(1)	12(1)

[a] U(eq) is defined as one-third of the trace of the orthogonalized $\mathbf{U}_{ij}$ tensor.

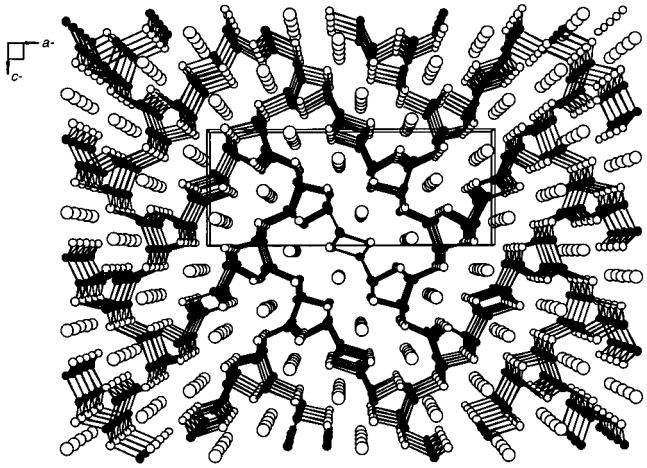

Figure 1. A [010] view of the orthorhombic unit cell of $BaGa_2Sb_2$. The Sb, Ga, and Ba atoms are indicated with small open, small filled, and large open circles, respectively.

Results and Discussion

Structure. The compound $BaGa_2Sb_2$ adopts a unique structure type with large tunnels running along the [010] direction. Ba^{2+} cations reside in the tunnels as shown in Figure 1. The projection along the *b*-axis illustrates that the tunnels are made from 26-membered rings. The basic building blocks of the network are $[Ga_2Sb_{6/3}]^{2-}$ units, where the six Sb atoms are coordinated to Ga−Ga dimers defining an ethane-like staggered conformation. These units share Sb atoms to form tubes with small four- and five-membered ring cross sections, Figure 2. The formal oxidation state of Ga is +2, while the three-coordinated pyramidal Sb atoms is assigned as Sb^{3-}; therefore, the formula is best represented as $Ba^{2+}[(Ga_2)^{4+}(Sb^{3-})_2]^{2-}$.

Conceptually, $BaGa_2Sb_2$ can be viewed as a 1 electron reduction product of GaSb. The added electrons in GaSb are expected to reduce Ga from 3+ to 2+ formal oxidation state. The strong tendency of Ga^{2+} to form Ga−Ga bonds probably prevents the compound from adopting a more ubiquitous structure type such as for example $ThCr_2Si_2$. The $[Ga_2Sb_2]^{2-}$ framework is isoelectronic to GaS which also has a unique structure with Ga−Ga bonds but adopts a lamellar motif.[14]

Group 13 compounds with the $[Ga_2Sb_{6/3}]^{2-}$ unit are rare. The mixed-valent framework in $Na_2[Ga_3Sb_3]$ and the structure of

(6) Pankove, J. I. *Optical Processes in Semiconductors*; Dover Publications: New York, 1976.
(7) (a) Hoffmann, R. *J. Chem. Phys.* **1963**, *39*, 1397. (b) Canadell, E.; Whangbo, M.-H. *Chem. Rev.* **1991**, *91*, 965.
(8) (a) Ren, J.; Liang, W.; Whangbo, M.-H. CAESAR 1.0 Primecolor Software, Inc., Cary, NC, 1998.
(9) (a) Wolfsberg, M.; Helmholz, L. *J. Chem. Phys.* **1952**, *20*, 837. (b) Ballhausen, C. J.; Gray, H. B. *Molecular Orbital Theory*; Benjamin: New York, 1965. (c) Basch, H.; Viste, A.; Gray, H. *Theor. Chim. Acta* **1965**, *3*, 458. (d) Basch, H.; Viste, A.; Gray, H. *J. Chem. Phys.* **1966**, *44*, 10. (e) Baranovskii, V.; Nikolskii, A. *Teor. Eskp. Khim.* **1967**, *3*, 527.
(10) *SMART*; Siemens Analytical X-ray System, Inc.: Madison, WI, 1994.
(11) *SAINT*, Version 4; Siemens Analytical X-ray System, Inc.: Madison, WI, 1994.
(12) Sheldrick, G. M. University of Göttingen, Göttingen, Germany, to be published.
(13) Sheldrick, G. M. *SHELXTL*, Version 5; Siemens Analytical X-ray System, Inc.: Madison, WI, 1994.
(14) Kuhn, A.; Chevy A. *Acta Crystallogr. B* **1976**, *32*, 983.

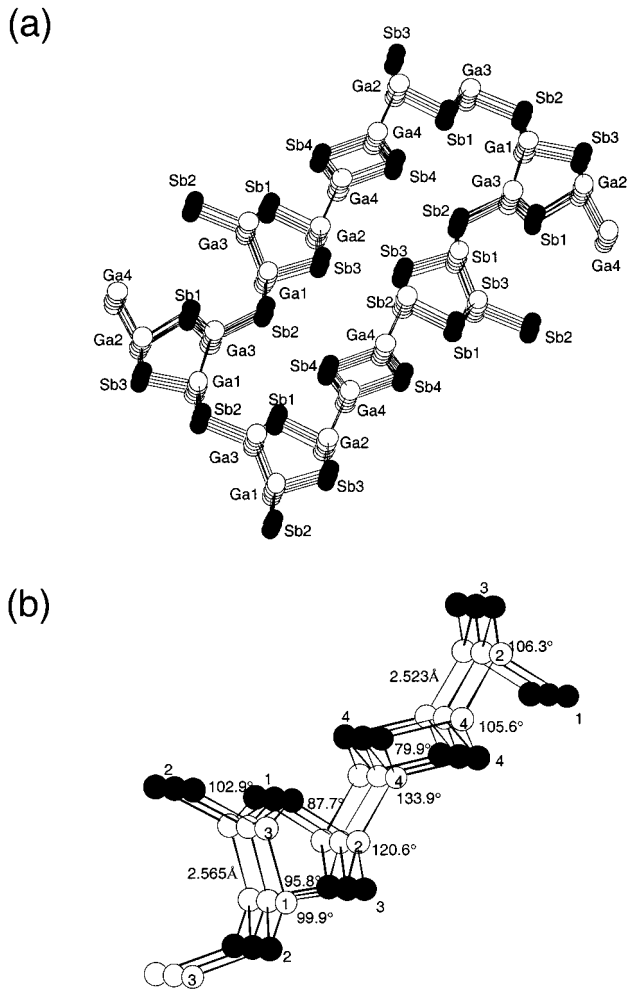

Figure 2. (a) Detailed view of the $[Ga_2Sb_2]^{2-}$ framework with atomic labeling. (b) Smaller section of the framework with selected bond lengths and angles. Black atoms are Sb.

$La_{13}Ga_8Sb_{21}$[15] are the only reported examples of pnictido group 13 metalate frameworks with Ga−Ga dimers. In $Na_2[Ga_3Sb_3]$, wavelike hexagonal nets of alternating Ga and Sb atoms are stacked and bound by Ga−Ga bonds to make three-atom-thick sheets. Therefore, this compound is layered with Na cations inserted between layers.[16] The anionic framework of $BaGa_2Sb_2$, however, is different from those of $Na_2[Ga_3Sb_3]$.

There are two crystallographically unique $[Ga_2Sb_{6/3}]^{2-}$ units in the structure of $BaGa_2Sb_2$ (Figure 2) with Ga−Ga bond lengths at 2.523(2) Å for Ga(4)−Ga(2) and 2.565(2) Å for Ga(1)−Ga(3). These bond lengths are comparable to the sum of covalent radii (2.52 Å) and also comparable to that (2.541 Å) found in $Na_2[Ga_3Sb_3]$ and $La_{13}Ga_8Sb_{21}$. The tetrahedral angles around the Ga atoms are in the range of 79.90(3)−133.91(5)°. Therefore, the local Ga atom geometry deviates strongly from the ideal tetrahedral bond angle. In $Na_2[Ga_3Sb_3]$, the corresponding angles (92.3−123.9°) also severely deviate from the ideal tetrahedral angle. This indicates that the coordination geometry around the Ga atoms is flexible and responds to the size of electropositive cations filling the framework. The Ga−Sb bond distances are in the range 2.665(1)−2.817(1) Å and appear to be regular covalent bonds. Selected bond distances and angles are given in Table 3.

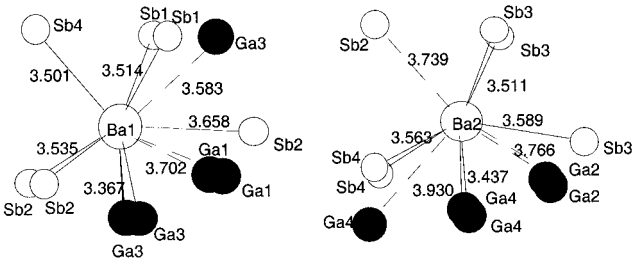

Figure 3. Coordination environment of the Ba atoms in $BaGa_2Sb_2$ where six Sb and five Ga atoms define the Ba cavity.

Table 3. Selected Bond Distances (Å) and Angles (deg) in $BaGa_2Sb_2$

Ga(1)−Ga(3)	2.5649(17)	Ga(3)−Sb(2)	2.7877(14)
Ga(1)−Sb(3)	2.7054(14)	Ga(3)−Sb(1) (×2)	2.6832(8)
Ga(1)−Sb(2) (×2)	2.7266(9)	Ga(3)−Sb(2)	2.7877(14)
Ga(2)−Ga(4)	2.5228(17)	Ga(4)−Ga(2)	2.5228(17)
Ga(2)−Sb(1)	2.6645(14)	Ga(4)−Sb(4) (×2)	2.7062(9)
Ga(2)−Sb(3) (×2)	2.7063(9)	Ga(4)−Sb(4)	2.8170(14)
Ba(1)−Ga(3) (×2)	3.3660(10)	Ga(2)−Sb(3)−Ga(2)	110.31(5)
Ba(1)−Ga(3)	3.5829(14)	Ga(4)−Sb(4)−Ga(4)	110.32(5)
Ba(1)−Sb(4)	3.5014(11)	Ga(4)−Sb(4)−Ga(4)	79.90(3)
Ba(1)−Ga(1) (×2)	3.7015(12)	Ga(3)−Ga(1)−Sb(3)	95.78(5)
Ba(1)−Sb(1) (×2)	3.5145(8)	Ga(3)−Ga(1)−Sb(2)	122.25(3)
Ba(1)−Sb(2) (×2)	3.5349(9)	Sb(3)−Ga(1)−Sb(2)	99.93(3)
Ba(1)−Sb(2)	3.6580(10)	Sb(2)−Ga(1)−Sb(2)	109.09(5)
Ba(2)−Ga(4) (×2)	3.4368(11)	Ga(4)−Ga(2)−Sb(1)	87.68(5)
Ba(2)−Sb(3) (×2)	3.5110(8)	Sb(1)−Ga(2)−Sb(3)	106.29(3)
Ba(2)−Sb(3)	3.5110(8)	Ga(4)−Ga(2)−Sb(3)	120.58(3)
Ba(2)−Sb(4) (×2)	3.5627(9)	Sb(1)−Ga(2)−Sb(3)	106.29(3)
Ba(2)−Sb(3)	3.5894(11)	Sb(3)−Ga(2)−Sb(3)	110.31(5)
Ba(2)−Sb(2)	3.7391(12)	Ga(1)−Ga(3)−Sb(1)	102.93(4)
Ba(2)−Ga(2) (×2)	3.7657(12)	Sb(1)−Ga(3)−Sb(1)	111.74(5)
Ga(2)−Sb(1)−Ga(3)	100.45(3)	Ga(1)−Ga(3)−Sb(2)	133.15(5)
Ga(3)−Sb(1)−Ga(3)	111.74(5)	Sb(1)−Ga(3)−Sb(2)	102.85(3)
Ga(1)−Sb(2)−Ga(1)	109.09(5)	Ga(2)−Ga(4)−Sb(4)	105.66(4)
Ga(1)−Sb(2)−Ga(3)	105.80(3)	Sb(4)−Ga(4)−Sb(4)	110.32(5)
Ga(1)−Sb(3)−Ga(2)	97.09(3)	Ga(2)−Ga(4)−Sb(4)	133.91(5)

The Ba atoms in the tunnels are surrounded by six Sb atoms and five Ga atoms (Figure 3). The coordination of the Ba(1) atoms is well described as a bicapped trigonal prismatic where the prism is defined by Sb(2) × 2, Sb(1) × 2, and Ga(3) × 2 with the Sb(4) and Sb(2) as the capping atoms. The Ba(2) atoms are surrounded by five Sb atoms at 3.5110(8)−3.589(1) Å and two Ga atoms at 3.437(1) Å, and all seven atoms define a monocapped trigonal prismatic geometry. The next-neighboring Sb(2), Ga(2), and Ga (4) atoms at 3.739(1), 3.766(1), and 3.930(1) Å are too far to be considered bonding. The bond distances of Ba−Sb and Ba−Ga calculated from metallic radii are 3.606 and 3.461 Å, respectively.[17] The Ba−Sb distances observed in $BaGa_2Sb_2$ are comparable to those found in $Ba_4In_8Sb_{16}$ and $Ba_7Ga_4Sb_9$.[18]

Electronic Structure. To understand the chemical bonding in this material, band structure calculations were performed on the $[Ga_2Sb_2]^{2-}$ framework. The band structure was calculated using the extended-Hückel formalism with the atomic orbital parameters of Table 4. Density of states (DOS) and crystal orbital overlap populations (COOP) were calculated on the basisi of 516 k points, and the results are shown in Figure 4. The calculations show that the valence states are completely filled and the Fermi level occurs at the energy gap, which suggests a semiconductor. The detailed energy dispersion analysis between

(15) Mills A. M.; Mar A. *Inorg. Chem*. **2000**, *39*, 4599.
(16) Cordier, G.; Ochmann, H.; Schäfer, H. *Mater. Res. Bull.* **1986**, *21*, 331.
(17) Pauling, L. *The Nature of the Chemical Bond*; Cornell Press: Ithaca, NY, 1960; p 403.
(18) Cordier, G.; Schäfer, H.; Stelter M. *Z. Anorg. Allg. Chem.* **1986**, *534*, 137.

Table 4. Atomic Orbital Parameters Used in Extended Hückel Calculations

atom	orbital	H_{ii} (eV)[a]	ζ_1[b]	C_1[b]
Ga	4s	−14.580	1.770	1.000
	4p	−6.7500	1.550	1.000
Sb	5s	−18.799	2.323	1.000
	5p	−11.700	1.999	1.000

[a] $H_{ii} = \langle\chi_i|H^{\text{eff}}|\chi_i\rangle$, $i = 1, 2, 3, ...$, the value approximated by valence-state ionization potential. [b] Single-ζ STO's.

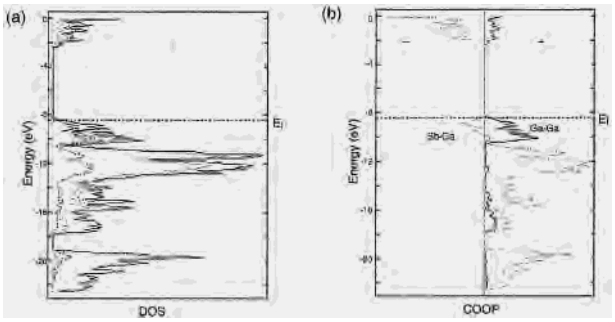

Figure 4. COOP and DOS curves for $BaGa_2Sb_2$. (a) Total DOS and projected DOS curves. The projectionS of Ga 4p (dash−dotted line), Sb 5p (dotted line), and total DOS (solid line) curves are shown. (b) COOP curves of Ga−Ga (solid line) and Ga−Sb (dotted line) interactions. It is implied that the structure is stabilized by covalent Ga−Ga interactions.

several high-symmetry points in the first Brillouin zone suggests that the energy gap in this compound is direct. Due to a known weakness of this calculation method, a quantitative comparison with the experimentally observed value is not possible.

The DOS plot in Figure 4a contains total densities together with projections for the Ga p and Sb p orbital contributions. The width of the valence band is relatively large at about 9.5 eV, which is due to the three-dimensional extent of the Ga−Sb interactions. The projected DOS show that the states near E_f are predominantly based on Ga 4p and Sb 5p orbitals mixed with some corresponding s orbital character. The block of states at lower energy (<-10.3 eV) are dominated by p orbitals of Sb, and the states above −10.3 eV are dominated by p orbitals of Ga. This is due to their electronegativity difference. According to the Zintl concept, the formal charge of the three-bonded Sb atoms can be assigned as Sb^0 and that of the four-bonded Ga atoms as Ga^-. Therefore, the band structure calculations also support $BaGa_2Sb_2$ to be structurally and electronically a Zintl phase.

In COOP plots, the projections for Ga−Ga and Ga−Sb bonds are shown in Figure 4b. Considering the lower oxidation state of Ga due to homonuclear Ga−Ga bonds, a slight antibonding character is anticipated on the Ga−Sb bonds. However, the states just below E_f are mainly from Ga−Ga bonding interactions, which suggests that the strong covalent Ga−Ga bonding contributes predominantly to the stability of the compound. Some of the Ga−Sb antibonding states just below the Fermi level are also filled suggesting some weakening of Ga−Sb bonding interactions.

Thermal and Spectroscopic Analysis. $BaGa_2Sb_2$ is stable at room temperature in air,[19] and it melts congruently at 767 °C provided care is taken to prevent the Ba from reacting with the container. $BaGa_2Sb_2$ is a narrow gap semiconductor as judged by the presence of a band gap observed spectroscopically in the IR region (4000−400 cm^{-1}) at 0.30−0.34 eV; see Figure 5. This is in agreement with the energy gap predicted by the band calculations. By comparison the diamond-like III−V semiconductor GaSb has a larger band gap of 0.69 eV at room temperature. The trend in band gap is similar in the $GaSe/Ga_2Se_3$ pair (1.1 vs 2.0 eV) in which a similar chemico−structural relationship exists. The GaSe structure contains Ga−Ga bonds, whereas the corresponding Ga_2Se_3 structure is a diamond-like tetrahedral structure (a defect variant of GaSb). Thus it would appear that the presence of homoatomic Ga−Ga bonds serves to substantially narrow the energy gap in comparison to compounds without such bonds.

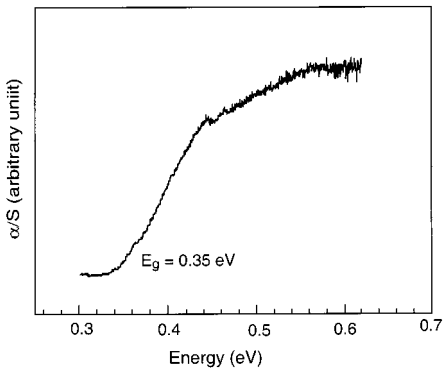

Figure 5. Infrared absorption spectrum of a polycrystalline sample of $BaGa_2Sb_2$. The energy gap is indicated.

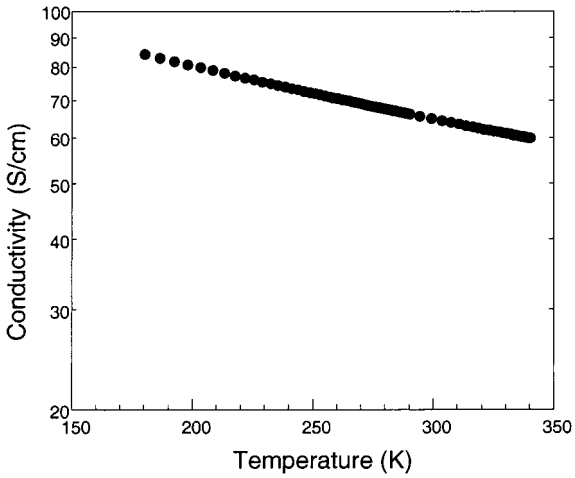

Figure 6. Temperature dependence of the electrical conductivity for a pellet of $BaGa_2Sb_2$.

Charge and Thermal Transport Measurements. The electrical conductivity and thermoelectric power of polycrystalline ingots of $BaGa_2Sb_2$ were measured as a function of temperature. The conductivity at room temperature is moderate at 65 S/cm (see Figure 6)[20] and only slightly lower than the ~135 S/cm found for $Ba_4In_8Sb_{16}$. The electrical conductivity does not vary greatly with temperature, consistent with a degenerately doped narrow gap semiconductor. The room-

(19) Interestingly, however, when the air-exposed sample is heated at ~500 °C, it slowly decomposes to Ga and unknown phases.

(20) (a) Dc electrical conductivity and thermopower measurements were made on a polycrystalline pellet with dimension of 2 × 2 × 5 mm^3. The pellet was sintered in evacuated graphite container at 500 °C for 2 h. Conductivity measurements were performed in the usual four-probe geometry with 60- and 25-μm gold wires used for the current and voltage electrodes, respectively. Conductivity data were obtained with a computer-automated system described in ref 19b. The Seebeck coefficients were measured between 290 and 450 K by using MMR SB-100 Seebeck Effect measurement system (MMR technologies, Inc.). (b) Kanatzidis, M. G.; McCarthy, T. J.; Tanzer, T. A.; Chen, L.-H.; Iordanidis, L.; Hogan, T.; Kannewurf, C. R.; Uher, C.; Chen, B. *Chem. Mater.* **1996**, *8*, 1465−1474.

temperature value of the thermoelectric power (Seebeck coefficient) for $BaGa_2Sb_2$ was about $\sim+65$ μV/K, and it slowly rises with increasing temperature. The positive thermopower values indicate that the material is a p-type (hole) semiconductor with holes residing in primarily Sb-based orbitals.

In conclusion, we have discovered a new Zintl phase, with Ga−Ga bonding and a unique channel structure formed by ethane-like Ga_2Sb_6 units. The large tunnels defined by the flexible Ga−Ga-based framework imply that different cations including rare-earth cations might be stabilized forming isostructural analogues.

Acknowledgment. Financial support from the Department of Energy (Grant No. DE-FG02-99ER45793) is gratefully acknowledged. S.-J.K. also acknowledges financial support from the Basic Research Program of the Korean Science & Engineering Foundation (Grant 2000-1-12200-002-3).

Supporting Information Available: Further crystallographic details and X-ray crystallographic files in CIF format. This material is available free of charge via the Internet at http://pubs.acs.org.

IC010069N